Wearable textile input device with multimodal sensing for eyes-free mobile interaction during daily activities

Sang Ho Yoon [a,*], Ke Huo [a], Karthik Ramani [a,b]

[a] School of Mechanical Engineering, Purdue University, West Lafayette, IN 47907, United States
[b] School of Electrical and Computer Engineering (by courtesy), Purdue University, West Lafayette, IN 47907, United States

HIGHLIGHTS

- Single-layer smart textile capable of capturing multiple sensing elements.
- Utilizing multimodal sensing to capture finger bending and pressing.
- Example applications with interaction design using proposed prototype.
- Performance evaluation under dynamic and eyes-free environments.
- Multitasking study to explore the prototype performance and perceived workload.

ARTICLE INFO

ABSTRACT

As pervasive computing is widely available during daily activities, wearable input devices which promote an eyes-free interaction are needed for easy access and safety. We propose a textile wearable device which enables a multimodal sensing input for an eyes-free mobile interaction during daily activities. Although existing input devices possess multimodal sensing capabilities with a small form factor, they still suffer from deficiencies in compactness and softness due to the nature of embedded materials and components. For our prototype, we paint a conductive silicone rubber on a single layer of textile and stitch conductive threads. From a single layer of the textile, multimodal sensing (strain and pressure) values are extracted via voltage dividers. A regression analysis, multi-level thresholding and a temporal position tracking algorithm are applied to capture the different levels and modes of finger interactions to support the input taxonomy. We then demonstrate example applications with interaction design allowing users to control existing mobile, wearable, and digital devices. The evaluation results confirm that the prototype can achieve an accuracy of $\geq 80\%$ for demonstrating all input types, $\geq 88\%$ for locating the specific interaction areas for eyes-free interaction, and the robustness during daily activity related motions. Multitasking study reveals that our prototype promotes relatively fast response with low perceived workload comparing to existing eyes-free input.

1. Introduction

Modern smartphone and wearable devices have laid the foundation for the pervasive computing in daily life. Nevertheless, they still adopt a touch-screen based input method due to the limitation of vision and biosignal based sensing
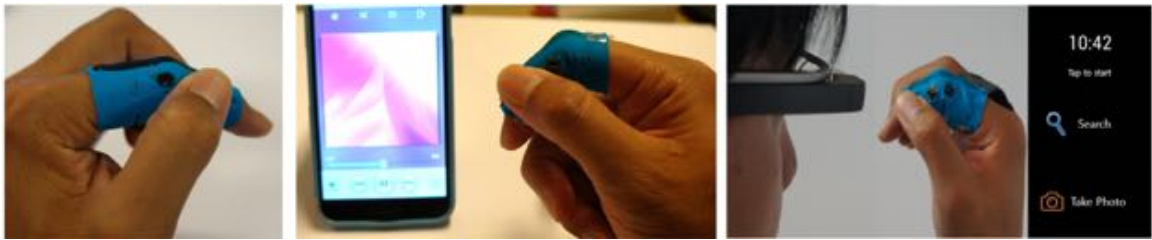
Fig. 1. Our prototype provides multimodal sensing through a single layer of textile to support eyes-free interaction during daily activities.

such as occlusions and motion artifacts [1,2]. The touch-based input requires users to switch their visual attention to the device while in use. However, splitting the attention during daily activities (exercising, driving, and working) causes falling, bumping, or traffic accidents [3]. Multimodal eyes-free interaction has a strong potential to prevent users from encountering dangerous situations by reducing cognitive/physical loads especially when access time for mobile devices is one of the key factor [4]. Wearables are found to be efficient in reducing the access time during the mobile interaction [5]. Thus, a multimodal sensing wearable device supporting eyes-free mobile input benefits users in terms of safety and accessibility.

Mobile interactions with various sensing techniques have drawn interest from researchers and developers to substitute the touch input [6]. Among them, smart textiles have been explored over the past decade as a solution for wearable devices due to the wearability and the soft texture [7]. By leveraging the material selection and fabrication, recent work has decreased the thickness of the smart textile while maintaining the performance [8]. However, previous works prefer implementing a single modal sensing for measuring passive inputs such as event recognition [9]. With a single sensing element, it is hard to provide a rich enough data to fulfill the input taxonomy needs of the state-of-art mobile devices. To this end, we explore a smart textile which is capable of supporting multimodal sensing capability as an input metaphor.

In mobile interaction, the hand embodies complex gestures with high precision and flexibility, and has been a key input mechanism. Within a hand, the most frequent interactions are created by the fingers [10]. By leveraging the use of fingers, previous works highlight performing rich interactions while maintaining a small wearable form factor as a pervasive input metaphor [11–14]. Although these techniques support pervasive computing, their approaches are not designed to work under dynamic environments including exercising, driving, or working. Moreover, the physical components used in these techniques make users hard to keep the natural hand posture while in use. To guarantee the performance in real environments, a finger-type device should properly function under various activities.

In this work, we present a multimodal sensing technique by merging strain and pressure sensors on a single layer of the textile (Fig. 1). Based on two different sensing modalities, we define two types of finger motions: finger pressing and bending. We employ a two-phase and a polynomial regression analysis to model the relationship between magnitudes of pressure and strain against applied finger pressing and bending. By using a multi-level thresholding, we capture different magnitudes from pressure and strain sensing. The swipe gesture is captured via the temporal position tracking algorithm. In total, 14 or more distinct inputs can be created with two-finger interaction. The prototype consists of elastic and soft materials to better preserve and improve the tactility and the wearability compared to attaching hard and rigid components. Use of elastic textile which induces pretension upon wear enhances the system robustness by correcting the initial offset values as well as providing stable fixation onto the body. Our initial results were first reported in *ACM UBICOMP 2014* and *ACM TEI 2015* [15,16]. Since then, we have completed interaction design process for demonstrating example applications. Extensive user studies have been carried out to evaluate the system performance during dynamic activity, eyes-free environment, and multitasking. Furthermore, we have compared the proposed prototype with other conventional input devices to get both quantitative and qualitative feedback from users. Our contributions include:

- Developing a single-layer smart textile capable of capturing multiple sensing elements during activities
- Utilizing multimodal sensing values from fingers to capture bi-directional swipe and different levels of finger bending and pressing
- Example applications with the finger-worn wearable prototype demonstrating rich eyes-free interactions
- User study to explore the performance of the proposed system under dynamic and eyes-free environments
- User study to explore the prototype performance in accuracy and reaction time as well as perceived workload comparing with existing input devices during multitasking

The rest of this paper is organized as follows. Section 2 discusses related work from the previous work. Section 3 describes the system design, preliminary experimental results, and example applications with corresponding interaction design. Section 4 offers user study results and implications from quantitative and qualitative data. Finally, conclusion and future work are discussed in Section 5.

2. Related work

Wearable input device: Wearable input devices provide significantly faster access time to interact with mobile devices [17]. With an advancement in sensor technology, small and powerful wearable input devices have been introduced.

Previous works implement wearable input system in various form factors including smart clothing, ring, necklace, wristband, and on-body [18–22]. Among sensing techniques, mechanical sensing is a promising approach to wearable input metaphors [23]. Mechanical sensing is intuitive since sensor values are created directly by the body movement such as finger bending, pressing, or rubbing. We differentiate our work by introducing a wearable device which demonstrates multimodal mechanical sensing including pressure and strain. In addition, our proposed work does not require attachment of rigid components around the sensing area and is designed to perform under the dynamic environment.

Smart textile: Textile sensors have been developed over the last two decades due to its comfort and softness. Previous research have demonstrated a pure textile pressure sensor as well as a strain sensor [8,24]. Utilizing conductive elastomers on a flexible substrate enabled a single layer fabrication of the strain sensor [25]. Shimojo et al. implements a single layer of a pressure sensor using carbon elastomer and metallic wires [26]. Recent works including Teleglove [27] and Beartek Glove [28] successfully embed sufficient numbers of input signals for the mobile interaction. However, these approaches require embedding sensors in multiple layers which diminish the tactility and comfort due to the stacked layer thickness [29]. Inspired from previous works, we integrate conductive elastomer and threads in a single layer of elastic fabric to provide a multimodal sensing capability that maintains both tactility and sensory comfort.

Finger based interaction: Interaction devices that can be worn on the finger have been highlighted because it represents human intent precisely with high flexibility [30]. Previously, various finger interaction tools are implemented with different sensing techniques and form factors. In the early work, a finger-worn controller is implemented by merging tactile buttons, capacitive touch sensor, and bend sensor [13]. However, it would be difficult to carry physical components along the fingers which prevents the users from maintaining the natural hand pose. During dynamic environment, it would increase false triggering from the capacitive touch sensor since the touch can be easily recognized with slight contact of other fingers. The magnetic sensing is used to track the finger position for interaction purpose [11]. Still, it is not reliable upon environmental magnetic field change and this method also requires instrumentation of magnet on the finger. The infrared marker detection and vision based approach are also introduced in finger based interaction [12,14]. Vision based approach has a limitation that it requires a line-of-sight view of hands and specific markers within the camera or optical sensing volume. Ring type devices are intuitive and easy to wear, but they generally require bi-manual operation and do not provide natural haptic feedback. Our approach suggests a finger operating wearable device which promotes using somatosensory tactility to support mobile interaction with a passive haptic experience.

Eyes-free interaction: In general, an eyes-free interaction is motivated to enhance the controllability while visually distracted from mobile devices [3]. There exist commercial eyes-free support input devices including wearable neckband headset and steering wheel controller. In recent works, eyes-free input methods have been suggested where users perform interaction without looking at the devices [18,31]. Suggested interactions are intuitive and eyes-free, but they either require extra motion to approach the sensing area or provide limited input gestures. With the multimodal feedback, the eyes-free interaction can perform as good as eyes-on interactions [32]. This indicates that an eyes-free interaction is suitable in applications where multimodal feedback information is naturally available. Our prototype supports an eyes-free interaction with reliable and rich interactions where the applications naturally provide feedback to users (e.g. controlling music player , hovering smartglasses user interface, and presenting slides). Furthermore, we perform multitasking user study with existing input devices to compare the performance and the perceived workload with our prototype.

3. System design

In the design of the prototype, the main goal is to achieve a finger-worn device that can perform rich and stable daily mobile interactions with comfort. To attain these goals, we implement the prototype with multimodal sensing in a single layer of textile. We explore the design rationale of our work and describe how the sensor is fabricated and the system is developed. The methodology of capturing different types of input are discussed with mathematical models and algorithms. The preliminary sensor evaluations to verify the multimodal sensing capability as well as dynamic environment feasibility are shown. We also demonstrate interaction design process with three example applications for an eyes-free approach.

3.1. Design rationale

For wearable devices, a placement of the system around human hand has shown the best performance and the user comfort [33,34]. In our work, the combination of thumb and inner index finger phalanx (towards thumb) is chosen as a main interaction area. The biomedical advantages of using index finger are two folds: a digit-wise independence and a pinch strength. The index finger shows a minimal passive motion due to the motions from other fingers [35]. The lateral pinch between thumb and index finger can exert more strength than any other pinching motion even including a chuck pinch [36]. This implies that the interaction using the thumb and the side of index finger phalanx can be regarded as a comfortable zone to perform physical interactions. Our choice also aligns with prior observations that these areas are the most frequently used during normal hand activities [10].

We implement sensing elements in a form of the smart textile. Strain and pressure sensing elements can understand basic finger motions including bending and pressing. Adopting these elements also frees users from the drawbacks of using other sensing techniques such as vision, that suffers from occlusions, and biosignal that is affected by motion artifacts. The
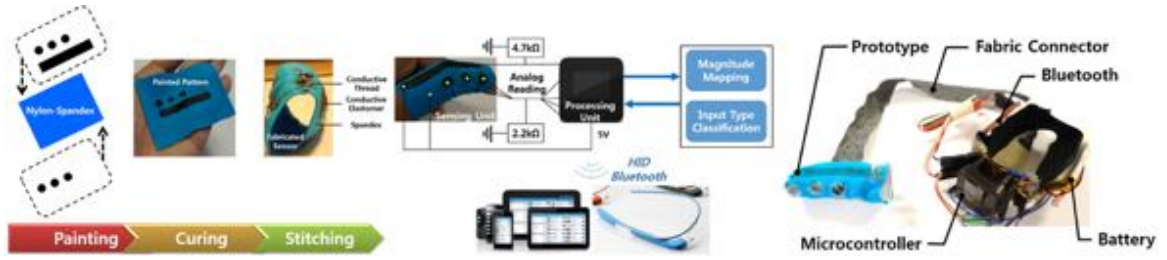
Fig. 2. Fabrication process (left), schematic workflow (middle), and our prototype (right).

textiles are chosen as base materials in order to maintain the passive haptic feedback and the sensory comfort of users. With a single layer of textile, we promote users to utilize somatosensory tactility under eyes-free mobile interaction. The sensory comfort is also entitled since no hard/rigid components are embedded in the prototype.

The development of mobile devices broadens the input taxonomy. A common touchscreen supports rich interactions through various input types including swipe, pinch, tap, and hold. To develop an input device which can accommodate current input vocabulary, the prototype should support rich enough inputs with natural interactions. It is hard to achieve the goal with a single sensing element. A synthesis of multiple sensing elements brings interaction richness which neither can provide alone. The suggested input metaphor consists of following unit interactions: (1) three different levels of finger pressing, (2) bending, (3) bi-directional swipe, and (4) simultaneous finger pressing + bending. These set of interactions are not rich enough to compare with the coordinate based touchscreen input. However, it provides rich enough interactions to control basic interface for the eyes-free mobile interaction.

3.2. Sensor design and hardware

Our prototype consists of an elastic fabric painted with conductive carbon elastomer [37] and conductive threads stitched on the fabric (Fig. 2). Nylon–Spandex fabric (80% Nylon and 20% Spandex) is selected due to the exceptional elasticity. The elasticity enables us to apply the pretension in the wearable setting to reduce sensor noises. The diluted conductive elastomer is painted using a stencil and a brush. We apply the conductive elastomer due to exceptional rebound elasticity (52%). The painted fabric is cured at 120 °C for 10 min. Combined Nylon–Spandex and customized ink exhibits a good piezoresistive properties (0.15 mm thick, resistance change of 50 Ω/in^2–40 kΩ/in^2 due to pressure, gauge factor of 5).

We conducted experiments on early fabricated samples to check the piezoresistive effect according to pressure and strain. The final design of strain and pressure sensing elements were based on the observed piezoresistive performance. For strain sensing, we tested several design candidates in terms of width and shape of the carbon elastomer. Although the high density of carbon composite is expected to increase the gauge factor, we observed decrease in fabric's elasticity with extensive elastomer stacking. As shown in Fig. 3(a), a 2 mm width exhibits the greatest gauge factor. However, 2 mm width often causes the crack during the usage and it was hard to align the center of upper finger with the thin design for proper usage. Thus, we choose 5 mm width to ensure the durability, to promote proper wear, and to keep acceptable performance. We also consider a 'V-shape' pattern in order to encourage wiring from the same side. Instead, we employ the straight line pattern which demonstrates higher gauge factor. The range of resistance change on strain sensing element (Fig. 3(a)) indicates that different levels of bending can be captured from raw sensor values. Meanwhile the pressure sensing design comprises of a 5 mm diameter circle which covers the typical size of a human fingertip. Fabricated pressure sensing area exhibits a maximum hysteresis of 15% which is similar to commercial force sensor resistor. Nevertheless, Fig. 3(b) implies that the hysteresis diminishes below 2% when applied pressure is larger than 1.5 N/cm^2. Since tactile triggers from users generally produce more than 1.5 N/cm^2, the hysteresis effect is negligible. The final design consists of a single line with 5 mm width and three spots with 5 mm diameter (Fig. 2) to measure strain and pressure respectively. While strain sensing is addressed with normal stitching, cross stitching into the front and back surfaces applies for pressure sensing [26].

Analog readings are transmitted to microprocessor through a customized fabric connector which is made of conductive thread on one end and metallic wires on the other end over spandex fabric (<0.2 Ω/cm). Instead of pure metallic wires, the customized fabric connector is used to keep the robust connection. In one end, the conductive threads are tied up with the prototype where the threads are wrapped around the metallic wires in the other end to hook up with microcontroller. The processing unit comprises a chip sized microcontroller [38] (ATmega328, 16 MHz clock speed), Bluetooth module (115200 bps), and 110mAh lithium-ion battery which provides 2.5 hours of operation with constant peak performance (Fig. 2). We select 2.2 and 4.7 kΩ resistors for pressure and strain sensing elements based on the voltage divider calculation:

$$\arg\max_{R} \left(\frac{R}{R_{sensor,max} + R} - \frac{R}{R_{sensor,min} + R} \right). \tag{1}$$

HID Bluetooth module passes input data via standard communication protocol which enables our system working with various platforms. The total weight of the system is under 50 g.

(a) Resistance change over different widths and strains.

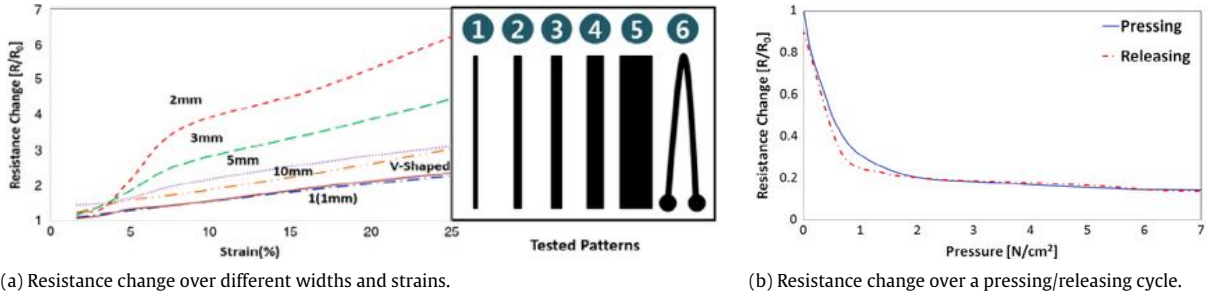(b) Resistance change over a pressing/releasing cycle.

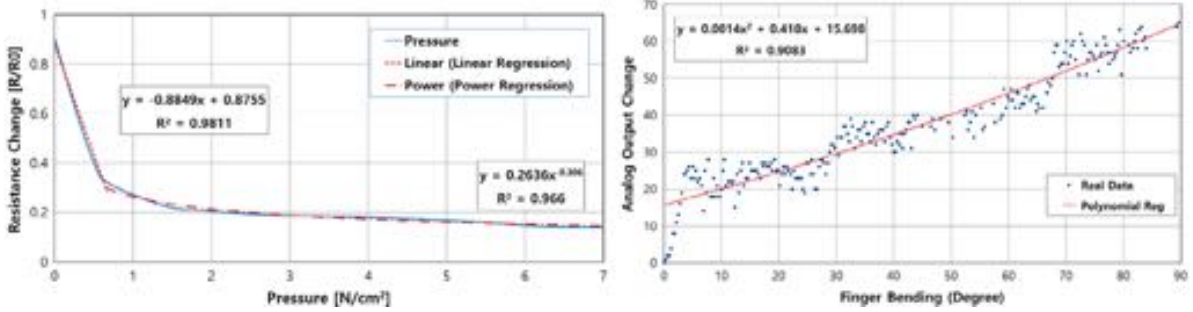Fig. 3. Strain and pressure sensing performance of fabricated smart textiles.

Fig. 4. Magnitude model using two-phase regression model for finger pressing (left) and polynomial regression model for finger bending (right).

3.3. Multimodal sensing implementation

The analog outputs behaviors against finger pressing and bending from the fabricated smart textiles are processed with two different regression models. Based on these models, we set global thresholds for different magnitude levels which is not subject dependent. Then, a temporal position tracking algorithm is applied to capture the bi-directional swipe gesture.

The bending and pressing magnitudes levels are defined by the regression analysis. Two-phase and polynomial regression models have been used for estimating magnitudes of pressure and strain [24,39]. The resistance changes are plotted against applied pressure and finger bending angle. The zero-calibration is performed before each trial to compensate for variations due to finger-worn conditions. For pressure, we use a two-phase regression model which can represent linear and exponential characteristics of the sensor behavior. Based on force gauge measurements with more than 20 samples, we come up with the threshold (0.7 N/cm^2) for two-phase model. For finger bending, we employ a polynomial regression model which represents magnitudes between $0°$ and $90°$ of proximal interphalangeal joint bending. Magnitude mappings are primarily carried out since mapped values are used as a reference in recognizing different levels of the input signal.

Two-phase Regression Model:

$$y_i = mx_i + b, \quad \text{for } x \leq 0.7 \text{ N/cm}^2 \tag{2}$$

$$y_i = \alpha x_i^{\beta}, \quad \text{for } x > 0.7 \text{ N/cm}^2 \tag{3}$$

Polynomial Regression Model:

$$y_j = \sum_{i=0}^{n} a_i x_j^i + \epsilon_j. \tag{4}$$

These magnitude models show an average accuracy of 97.3% (pressing) and 90.6% (bending). Plots illustrate the raw data and the developed regression models (Fig. 4).

We utilize these magnitude models to capture different inputs. In this work, we dissect pressure and bending magnitudes into three regions which can distinguish more than an on/off status. The segmentation levels can be adjusted according to applications. We employ a temporal position tracking method to detect the swipe gesture and differentiate it from discrete finger pressing. If users trigger the two farthest painted spots with the lowest level of pressure input, the algorithm counts the time gap between the two events. The whole event is recognized as a swipe gesture only if the time gap falls within a specific constant for which we use 0.5 s (<0.1 m/s). Total of 14 different inputs are provided including three different levels of finger bending and pressing as well as bi-directional swipe gesture.
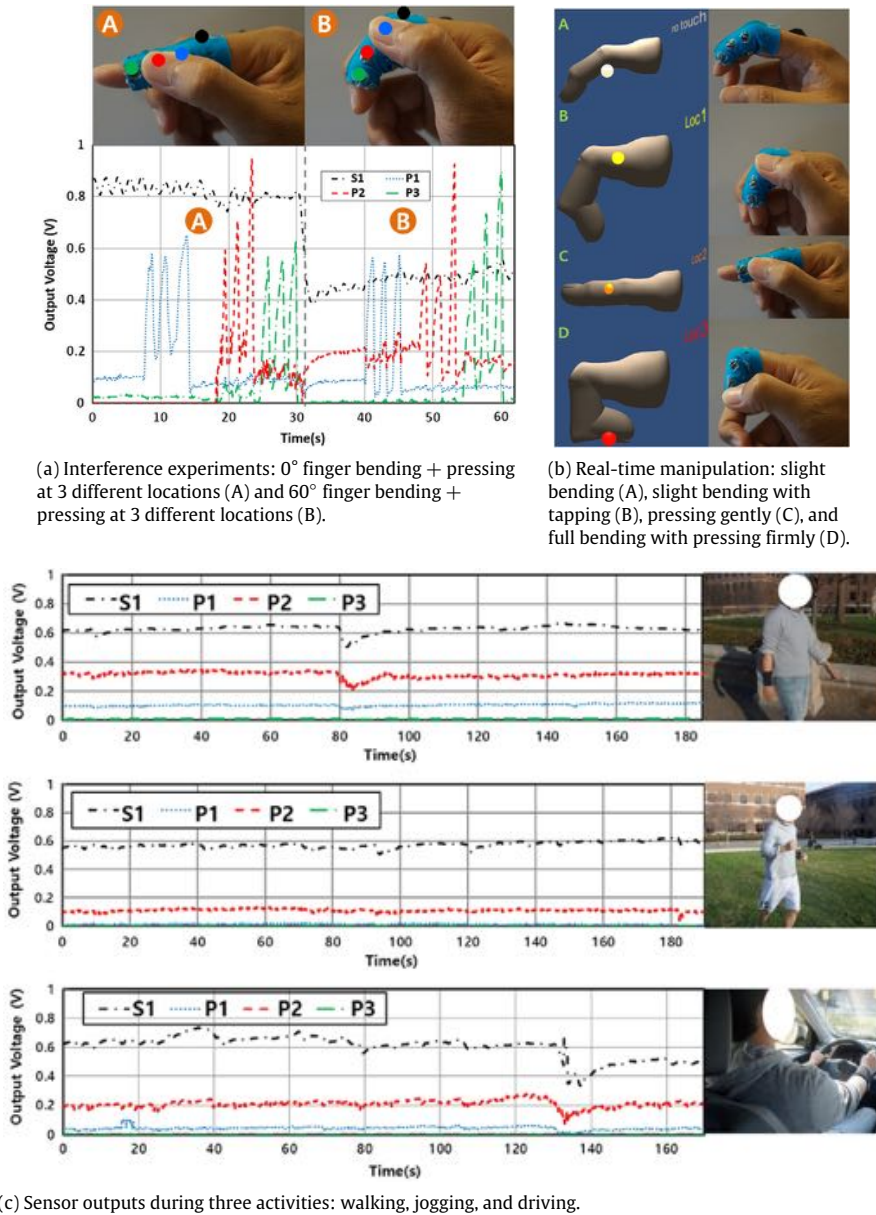
(a) Interference experiments: 0° finger bending + pressing at 3 different locations (A) and 60° finger bending + pressing at 3 different locations (B).

(b) Real-time manipulation: slight bending (A), slight bending with tapping (B), pressing gently (C), and full bending with pressing firmly (D).

(c) Sensor outputs during three activities: walking, jogging, and driving.

Fig. 5. Preliminary experiments with the prototype for feasibility test in daily mobile interaction.

3.4. Preliminary sensor evaluation

We carry out initial tests on pressing and bending to investigate the discrete and simultaneous multimodal sensing capability of fabricated smart textile. We assume that each sensing element performs without physical crosstalk if we isolate them to discrete faces of a finger. In the tests, we put pressure on different painted spots while straightening and bending the finger. As shown in Fig. 5(a), strain values fluctuate within a small range due to the natural finger motion while pressing each spot. The normalized output of the strain and pressure sensor outputs stay within ± 0.1 when they are not intentionally activated. The result indicates that the interference between sensing elements is negligible. The applied painted spot size is found out to be reasonable since fingertip only triggers intended sensing element.

To verify the functional feasibility during daily mobile interaction, we also examine the prototype in three dynamic activities: walking, jogging, and driving. The pretension from the elastic band provides a stable fixation between the prototype and the index finger. This diminishes the sensor noises caused by dynamic motions as shown in Fig. 5(c). The strain values show high noise intensity which comes from the natural passive motions during swinging the upper arm. Also, pressure values occasionally drop when the prototype loses contact with the finger. By setting bigger threshold intervals
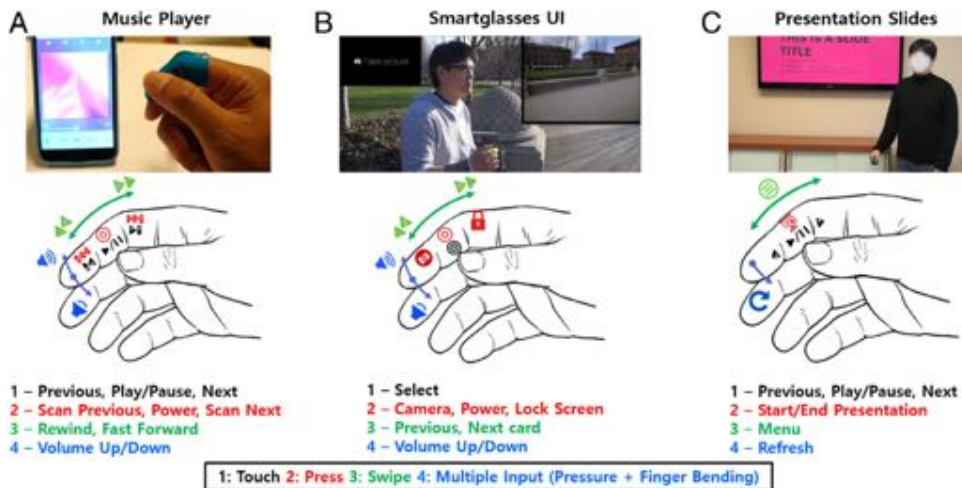
Fig. 6. Example applications with corresponding interaction mapping for controlling (A) smartphone music player (B) smartglasses user interface, and (C) presentation slides. All controls are based on four input metaphors: (1) Touch, (2) Press, (3) Swipe, and (4) Press + Finger Bending.

for the strain sensing and filtering sudden pressure drop, these noises are eliminated. The virtual fingers are animated to check the real-time performance of the prototype in a wireless setting (Fig. 5(b)). The preliminary experiments and real-time demonstration ensure the performance of multimodal sensing capability and the robustness during daily activities.

3.5. Interaction Design Example

The prototype enables the following natural finger motions as input methods: inter-finger pressing (pressure sensing), finger bending (strain sensing), and inter-finger rubbing (swipe). In this section, we design interactions using the above finger motions to embody an eyes-free interaction. Finger motions are naturally used with mobile devices and computers. Thus, finger motions can easily represent basic functions such as selection, hovering, and intensity control.

There are three distinct pressure sensing areas placed on the side of the index finger. This area has biomechanical and ergonomic advantages for finger interaction accuracy and accessibility. Thumb fingertip covers the entire area of the side of the index finger and it is hard to miss this area for pressing due to human's somatosensory tactility and proprioception. We implement a low-profile simple 3-button user interface (UI) on the side of the finger. Since the prototype is capable of sensing three different levels of pressure magnitude, multiple-layer input sets are applied which provides us with the ability to support nine different inputs. The maximum number of functions increases with adding more intervals based on the finger press, but it expects to increase both complexity and physical/cognitive load. The swipe gesture has been widely used in existing devices such as flipping pages in e-book, skipping to previous/next song in multimedia player, and hovering through the UI menu. Thus, we provide bi-directional swipe to be mapped with these inherent conventional functions.

Finger bending has been generally used as a common gesture for sliding, scrolling, and scaling UI. People bend their index fingers when they scroll the wheel for skimming through web pages or documents [40]. In previous research, bending involved pinching is also mapped to the slider mechanism as a level controller [41]. We select the finger bending as a key component to manipulate the slider UI.

The prototype provides concurrent sensing of finger bending and pressing. For the prototype, a false trigger might result an issue since the prototype is designed to be used under dynamic environments. In order to prevent this, the interaction should encompass the user intent which cannot be easily triggered by passive human motions. We suggest using 'Hold' gesture as a switch to initialize the interaction. After initialization, the finger bending motion is incorporated as a slider. Moreover, different types of intensity control can be embedded at each location with distinct pressure sensing locations.

3.6. Example applications

In our work, we implemented three applications: controlling smartphone's music player, smartglasses user interface and presentation slides. All applications naturally support auditory/visual feedback upon user's input. With the passive tactile feedback from a low-profile sensor, suggested applications provide a robust eyes-free interactions. In our examples, we directly pair it with existing devices without any software or hardware modifications. This ensures the compatibility of our prototype for general input device. Demonstrated examples envision that existing and future wearables, mobiles, and digital products will get benefits from new interaction affordance provided by our prototype.

The eyes-free mobile interaction assists the user during daily activities in both indoor and outdoor. Shifting from traditional mobile phone to smartphone makes people spend more time on looking and touching the screen [42]. This

puts users in situations where their attention is split such as reckless driving or careless walking. We provide rich enough interactions to control music player's overall functions including initiate/exit music player, play/pause, fast forward, rewind, scan previous/next song, and volume up/down. Even though the prototype has a great efficiency under an eyes-free environment, it can be also applied in general situations. If the users cannot operate touchscreen (e.g. wet/stained finger, touchscreen malfunction, exercising), it provides a basic graphic user interface (GUI) control function including left/right/up/down cursor movement, selection, back/cancel, and home functions. We demonstrate a stable and rich interaction tool that works during various activities with digital devices including mobile and computer.

As a wearable input device, the prototype brings a new input metaphor by combining it with existing wearables. Although people generally use built-in trackpad or touchscreen, our prototype provides richer input methods. Currently, people interact with Google Glass™ using an embedded track pad on the frame which requires noticeable hand movement by nearby people. Controlling through fingers emphasizes the private aspect of interaction where user's intent to use the device is less noticeable. The existing track pad in Google Glass™ enables only few input mechanisms including left/right swipe, select/cancel using touch and power on/off with a button. Although smartglasses adopts the voice control for executing complex task, people are not in favor of exposing their voices to the public. As shown in the smartphone application, we provide plenty of mapped functions to control the general GUI. Thus, it has a high potential to improve the social acceptability by providing rich taxonomy for inputs.

Our prototype also supports existing desktop or laptop as an auxiliary input device. Keyboard and mouse are general input devices with high accuracy and speed. However, people uses extra input device based on different usage context. For example, people often use wireless laser presenter/pointer or gesture control arm band [43] for the presentation during meeting or conference. As shown in the figure (Fig. 6), controlling presentation slides is achievable using our prototype.

Our examples imply that the prototype can be used in various daily activities during exercising, driving, and working. The prototype provides an always-available and easily approachable control mechanism which is embodied by finger motions. Our main design space would be using the prototype with the application which requires less-context specific control. The reason is that the eyes-free interaction aims for less physical/cognitive load. Thus, the prototype is more suitable to deal with the context with less steps to accomplish a task such as reacting to incoming call, controlling music player, and manipulating slides. With display-support wearables like smartglasses, our prototype still achieves full control under the context-specific application since smartglasses generally provides similar input mechanism such as touch and swipe. In this case, our prototype expects to bring down the social awkwardness of using the smartglasses by providing subtle motion during input triggering.

4. User study

In this section, we carry out two users studies: performance evaluation and multitasking study. In performance evaluation, we examine the overall system performance of our prototype. The purpose of multitasking study is to explore the multitasking performance and perceived workload in respect to existing eyes-free and eyes-on input devices.

4.1. Performance evaluation

We evaluate the system accuracy from users on using proposed application with the prototype. We perform two sets of evaluation: (1) Basic functionality accuracy in a static environment and (2) Pressure trigger accuracy in dynamic and eyes-free environments. For the evaluation, we intentionally design algorithms based on a simple thresholding using raw sensor values. Although machine learning can improve the performance, here we test the raw data usability and performance. For all studies, we had a practice session where participants play with the prototype using the graphical representation as shown in Fig. 5(b). In average, participants were ready for the study within 10 min of the practice. All users were able to reach all sensing spots provided by our prototype. The finger bending intensity to reach each pressure sensing spot was different from users, but all users showed that they had to bend their fingers in order to reach outer most spot.

4.1.1. Basic performance evaluation

To check the accuracy of the basic functionality, we conducted a small session to confirm the input classification performance in a static environment. It involved 7 participants with a mean age of 27 (all right-handed). We asked them to execute every input type designed in our prototype (14 classes) 10 times including different levels of pressing and bending as well as swiping in both directions. The zero-calibration was carried out with a straight finger posture prior to each test.

Fig. 7 illustrates the confusion matrix of different input types. Pressing and bending magnitude detection exhibited an average accuracy of 97% and 92% respectively while swipe gesture detection gave 80% accuracy. Less accuracy was observed in swipe gestures due to differences in swipe velocities among users. The result indicated that the prototype performs well in a static environment. This leads us to perform next evaluation in more complex scenario involving dynamic and eyes-free environments.

4.1.2. Dynamic eyes-free performance evaluation

In this evaluation, we recruited another 8 participants with mean age of 27.5 to evaluate the performance under dynamic and eyes-free environments (all right-handed). We collected raw sensor values for three different tasks: (1) Physical
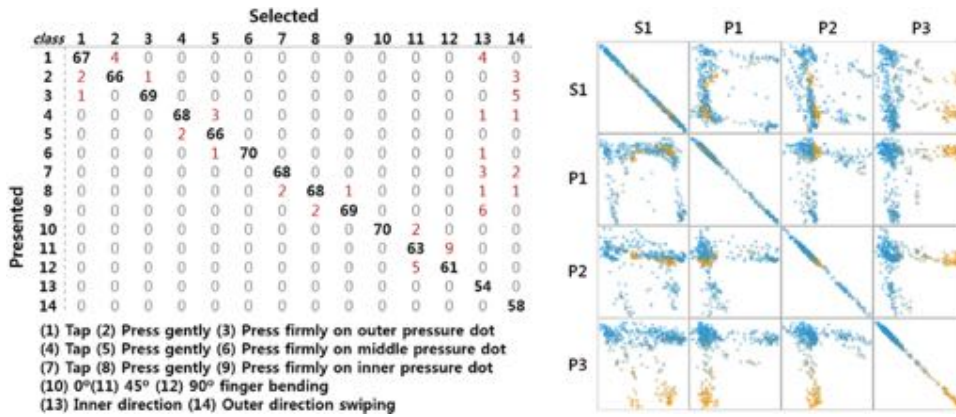
class	1	2	3	4	5	6	7	8	9	10	11	12	13	14
1	67	4	0	0	0	0	0	0	0	0	0	0	4	0
2	2	66	1	0	0	0	0	0	0	0	0	0	0	3
3	1	0	69	0	0	0	0	0	0	0	0	0	0	5
4	0	0	0	68	3	0	0	0	0	0	0	0	1	1
5	0	0	0	2	66	0	0	0	0	0	0	0	0	0
6	0	0	0	0	1	70	0	0	0	0	0	0	1	0
7	0	0	0	0	0	0	68	0	0	0	0	0	3	2
8	0	0	0	0	0	0	2	68	1	0	0	0	1	1
9	0	0	0	0	0	0	0	2	69	0	0	0	6	0
10	0	0	0	0	0	0	0	0	0	70	2	0	0	0
11	0	0	0	0	0	0	0	0	0	0	63	9	0	0
12	0	0	0	0	0	0	0	0	0	0	5	61	0	0
13	0	0	0	0	0	0	0	0	0	0	0	0	54	0
14	0	0	0	0	0	0	0	0	0	0	0	0	0	58

(1) Tap (2) Press gently (3) Press firmly on outer pressure dot
(4) Tap (5) Press gently (6) Press firmly on middle pressure dot
(7) Tap (8) Press gently (9) Press firmly on inner pressure dot
(10) 0°(11) 45° (12) 90° finger bending
(13) Inner direction (14) Outer direction swiping

Fig. 7. Confusion matrix of different input types. Rows indicate presented inputs and columns refer to selected inputs (left). Correlation Matrix from a participant showing the independent relationship among each sensing element (right).

class	P1 (Outer)	Selected P2 (Middle)	P3 (Inner)
P1 (Outer)	57	5	0
P2 (Middle)	3	57	5
P3 (Inner)	3	9	63
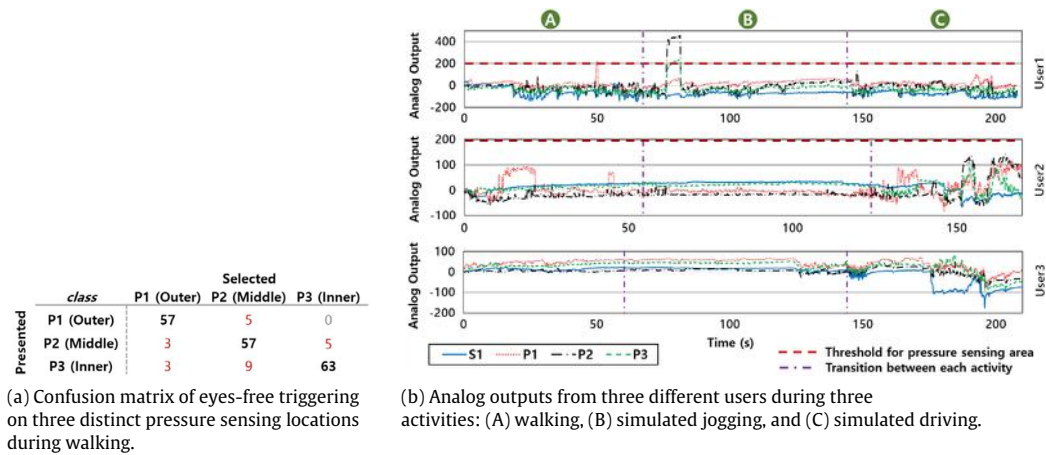
(a) Confusion matrix of eyes-free triggering on three distinct pressure sensing locations during walking.

(b) Analog outputs from three different users during three activities: (A) walking, (B) simulated jogging, and (C) simulated driving.

Fig. 8. Evaluation results on the performance of the proposed prototype in (a) eyes-free condition and (b) dynamic environments.

interference check during normal usage, (2) Perform dynamic activities without input trigger (walking and simulated running/driving), and (3) Eyes-free input control. Through these tasks, we evaluate the sensor interference with real users, unintentional triggers during dynamic motions, and eyes-free performance on control using the prototype.

For the first task, users were asked to trigger three pressure sensing elements while straightening and 60° bending. We visualize sensor outputs of one participant with a correlation matrix in Fig. 7. This matrix illustrates that each sensing element does not interfere with other sensors demonstrating the independence relationship of each sensing element. Similar results were observed from all other participants. The result affirms that each sensing element works robustly without physical interference for various users with different finger sizes.

In the following task, users were told not to trigger any inputs during walking, simulated running by swinging the upper arm, and simulated driving by manipulating the steering wheel on the desk. Our aim was to check the unintentional pressure sensor triggering. We set analog thresholds of 200 as a triggering the inputs which was used for the lowest level of pressure detection in our previous application. Fig. 8(b) illustrates that three different users barely trigger pressure based input over the course of different activities. Results for all other users show high consistency. The simulated driving activity (last region in each graph) created the most noise values among all activities. From our observation, it was mainly due to user's habitual motion behavior such as holding a steering wheel at skewed positions. However, these noises were not large enough to pass over the threshold. For strain sensing, the outputs exhibited fluctuations caused by natural passive motion. In order to prevent accidental triggering from finger bending, a switch to initialize the finger bending interaction should be embedded as suggested in the *Interaction Design Example* section. The results indicate that the motion artifact does not cause the false-trigger during daily activities.

In the last task, we asked users to trigger three distinct pressure sensing areas at least 5 times each with a random order. Users performed the task while they were walking. The user intentions were confirmed manually as the users notified which element they intended to trigger after each action. The confusion matrix shows the accuracy in an eyes-free environment for three different pressure spots (Fig. 8(a)). The average accuracy of eyes-free triggering is 88%. Based on the results, we

Table 1
Stimulus and response modality for primary and secondary tasks.

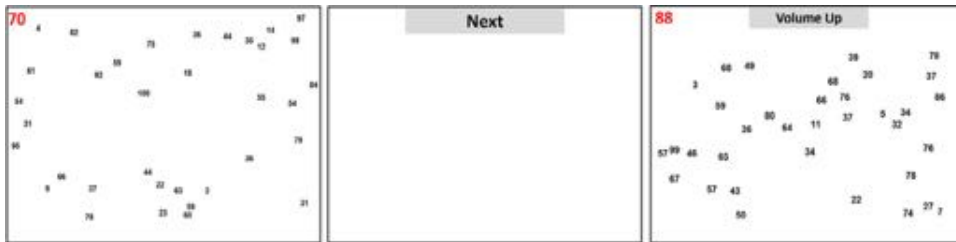|	Task	Stimulus	Response
Primary	Visual screening task	Visual	Vocal
Secondary	Phone	Visual	Visual+Motor
	Bluetooth headset	Visual	Motor
	Steering wheel	Visual	Motor
	Textile	Visual	Motor

Fig. 9. Primary task level "Hard" with 35 two-digit numbers (left), secondary task instruction (middle), and dual task with both primary and secondary task (right).

conclude that the 3-button UI for eyes-free interaction is feasible to implement in the mobile interaction. We did not explore the eyes-free performance of finger bending since it is designed to be used for a slider mechanism rather than selection tasks.

Above results support that the prototype is composed of independent pressure and bending sensing elements. Although the user rarely triggered the pressure sensing elements due to their habitual behaviors, the prototype also exhibited robustness against general dynamic motions. The eyes-free performance of 3-button UI implies that locating more than 3 buttons on a single finger will not provide enough accuracy for the mobile interaction ($< 88\%$).

4.2. Multitasking evaluation

The purpose of this study is to explore how user performance in terms of accuracy and reaction time differ under visually distracted condition. We compare with other input devices which support both eyes-free and non eyes-free feature. As suggested in Schumacher's study [44], we adopted independent stimulus–response (S–R) channel for primary and secondary task rather than using single S–R channel. To avoid modality conflict, we used vocal response for the primary task and motor response for the secondary task (Table 1). All tasks were based on visual stimulus since auditory stimulus will interfere with the vocal response from the primary task. We have two hypotheses for this evaluation: Since our prototype encourages use of proprioception from fingers, (1) users will get less affected by the visual distraction on secondary task performance and (2) less overall workload while maintaining primary task performance.

4.2.1. Setup

For study setup, we divided tasks into two groups: primary and secondary. We considered the interaction with the world as the primary task and interaction with input devices as the secondary task. Previously, multitasking evaluation for wearable tactile alert perception has been done thoroughly [45]. The purpose of previous study was to measure the performance of the alert perception during visual distractions. This aligned with our study goal where we aimed to find the input device performance under visual distractions. Therefore, we adopted same visual screening tasks with three difficulty levels proposed by previous work (9, 25, and 35 stimuli). The primary task was a forced-choice visual screening task like shown in Fig. 9. Participants were instructed to find the target stimuli (a two-digit red number on the top-left corner) among other stimuli (black number between 0–99) within five seconds. Then, the participants were asked to respond "Yes" for stimuli detection or "No" for missing target stimuli. The location and combination of stimuli were randomly mixed for each trial and half of the trials contained target stimuli. The trials for each task were in random order.

For secondary task, we chose music control task since it is general mobile tasks in various environments including driving, running, walking, or sitting. As shown in Fig. 10, the different setup and input mappings (play/pause, power, previous/next song, and volume up/down) were used for simulating different environments. We chose three conventional input devices to compare with our prototype: smartphone with touch input, steering wheel with buttons (Gaming Steering Wheel), and Bluetooth headset with buttons (LG Tone Pro). These devices were chosen since they represent conventional input device to control the music player in different settings. The flag for the secondary task was given visually like shown in (Fig. 9). Based on given instruction, the participants required to trigger the given target stimuli. During the user study, we named our prototype as "Textile" for easy reference.
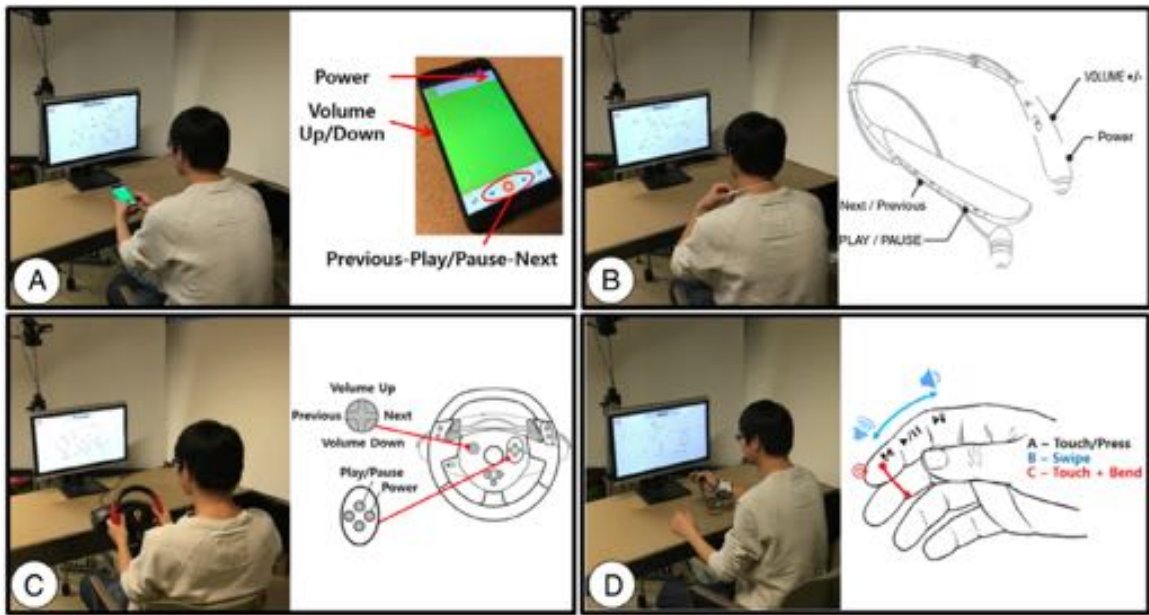
Fig. 10. Test setting for dual task with different input devices including (A) phone (B) Bluetooth headset (C) steering wheel, and (D) textile with same input functions (volume up/down, play/pause, previous, next, and power). Mappings are demonstrated on the right figures.

Table 2
Conditions for all tasks in the main session (1: Easy, 2: Moderate, 3: Hard, P: Phone, H: Bluetooth headset, T: Textile, S: Steering wheel).

ID	Single Task							Multi-task											
	S1	S2	S3	S4	S5	S6	S7	D1	D2	D3	D4	D5	D6	D7	D8	D9	D10	D11	D12
Primary	1	2	3	-	-	-	-	1	2	3	1	2	3	1	2	3	1	2	3
Secondary	-	-	-	P	H	T	S	P	P	P	T	T	T	H	H	H	S	S	S

We recruited 9 participants in this study with a mean age of 28.6 (all right-handed). Participants had average of 5 years with smartphone experience. 6 users had experience with Bluetooth headset and 5 users had used steering wheel with buttons. The test duration was approximately 90 min.

4.2.2. Procedure

We used a within-subject design method in this evaluation since individual performance varies in controlling different input devices. The study comprises of practice and main sessions. In the practice session, three trials for each level of the primary task and for each device in the secondary task were carried out as a single set to reduce the learning effect.

In the main session, the accuracy and reaction time for both primary and secondary task were collected through logged data from input devices and audio–video recordings. As shown in Table 2,there were total of 19 task conditions. In 'Single' tasks, primary and secondary tasks were measured individually (S1-7). In dual task conditions, however, each input device was paired with different levels of visual distraction (D1-12). For each condition, the number of trials were 30 and 15 for primary and secondary task, respectively. The total trials were 4050 trials (30 trials × 9 users × 15 conditions) and 2160 trials (15 trials × 9 users × 16 conditions) for the primary and the secondary task. The interval between the primary task was 5 s. The interval between the secondary task was between 7–13 s with average of 10 s. To prevent user fatigue, we offered 2 min break every 10–15 min.

After all sessions, we took workload assessment survey based on NASA-TLX. We also received user comments on using tested devices as input methods in various environments.

4.2.3. Task result

In this section, results are divided into two folds: primary task and secondary task. For primary task, the independent variables are difficulty of visual distractions and different input devices(no input device, smartphone, Bluetooth headset, steering wheel, and textile). In secondary task, the independent variables are different types of input devices and types of task (single task and dual task with different visual distraction difficulties).

The effects of different visual distraction difficulties on the primary task performance in both accuracy and reaction time are statistically significant using a one-way ANOVA (Fig. 11, $p < .01$). As the visual distraction gets harder, the accuracy and time reaction performance decrease. Although most users came up with the strategy to prioritize the primary task to manage multitasking, we observed that participants prepared for the input triggering while carrying out the primary task.
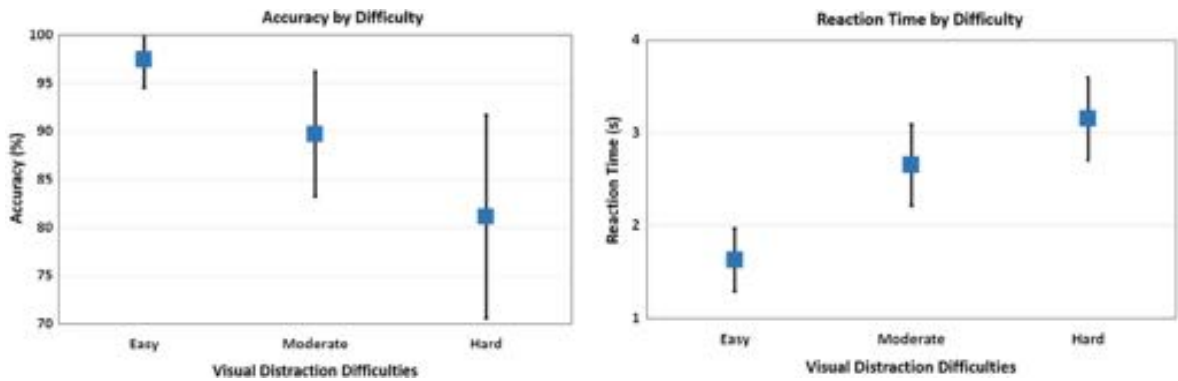
Fig. 11. Primary task by visual distraction difficulties: Accuracy (left) and Reaction Time (right).
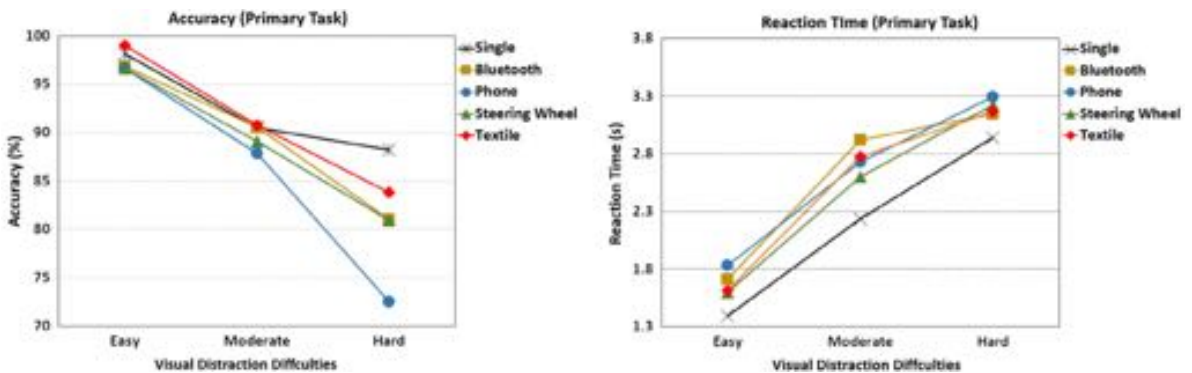

Fig. 12. Primary task results: Accuracy (left) and Reaction Time (right).

Fig. 12 shows accuracy and reaction time for the primary task during single and dual task conditions. As expected, single task performs the best in respect to both accuracy and reaction time due to low cognitive load comparing to dual task. The primary task accuracy using smartphone is significantly different from other input devices. We assume that the requirement of an eyes-on interaction from the phone adds task loads. The primary task accuracies using Bluetooth headset, steering wheel, and textile are not significantly different. However, participants show much higher miss rate (participants skipped the trial without response) when using Bluetooth headset (10%) comparing to steering wheel and textile (<5%). The reaction times are not significantly different across all input devices for the primary task.

In the secondary task, we look at the accuracy and reaction time for each input device during single and dual task conditions (Fig. 13). We perform a one-way ANOVA to compare the significant difference. The effects of the multitasking on accuracy are statistically significant for phone and steering wheel ($p < .05$), but not significant for Bluetooth headset ($p > .05$) and textile ($p > .4$). The effect of the multitasking on reaction time is statistically significant for phone, Bluetooth headset, and steering wheel ($p < .01$), but not for the textile input ($p > .15$). This implies that the textile input device is less susceptible to multitasking while all other input methods perform worse in either category (accuracy and reaction time) during multitasking.

Fig. 14 represents accuracy and reaction time for secondary task for all input devices during single and dual task conditions as well as for different visual distraction difficulties. The textile input device shows the least maximum accuracy due to the prototype limitation as discussed in previous section. However, the accuracy drop rate is more evident in phone, Bluetooth headset, and steering wheel during dual tasks. In addition, the average reaction time from single task to dual task increases more with the phone (55%), Bluetooth headset (40%), and steering wheel (63%) than the textile input (17%).

4.3. Workload assessment & user feedback

Following the main session, all participants filled out NASA Task Load Index rating sheet [46] for each tested input device. By including conventional input devices supporting both eyes-free and eyes-on interactions, we obtain the comparable perceived workload with our prototype. Moreover, participants gave us verbal/written feedback about their experiences with different devices in multitasking scenario.
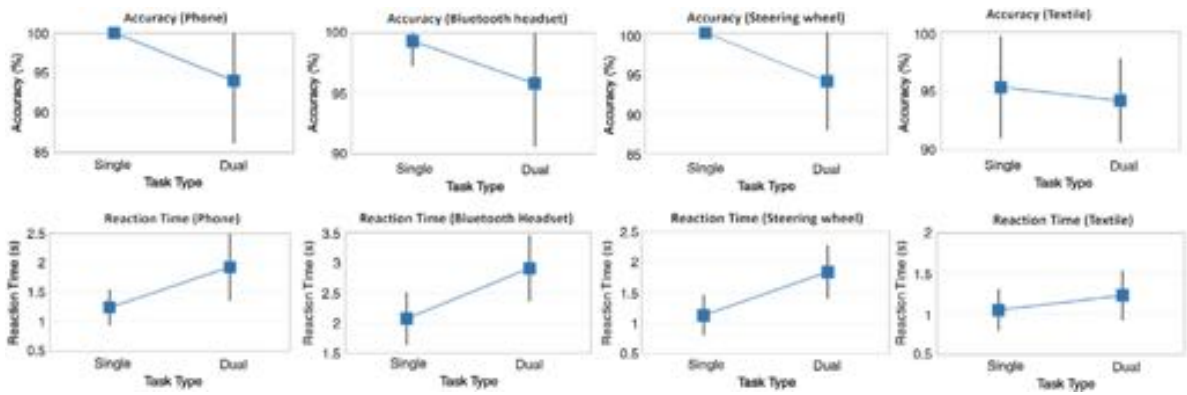
Fig. 13. Accuracy and reaction time for different input devices in single and dual task conditions: Phone, Bluetooth headset, Steering wheel, and Textile (left to right).
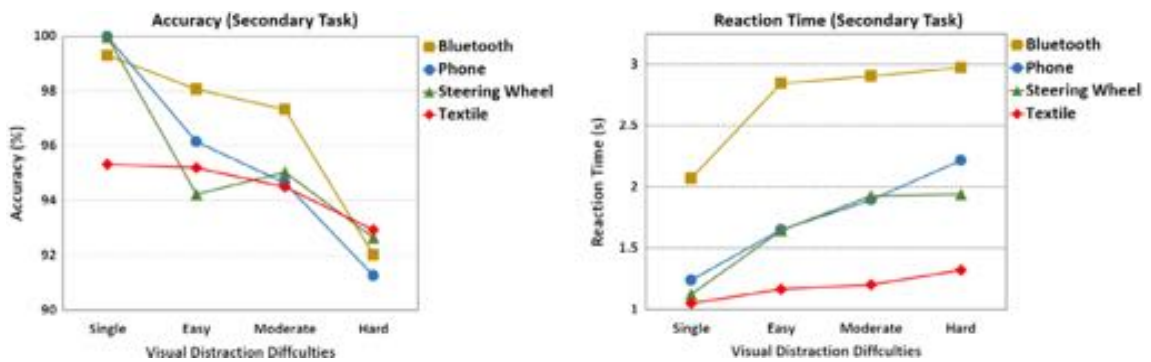

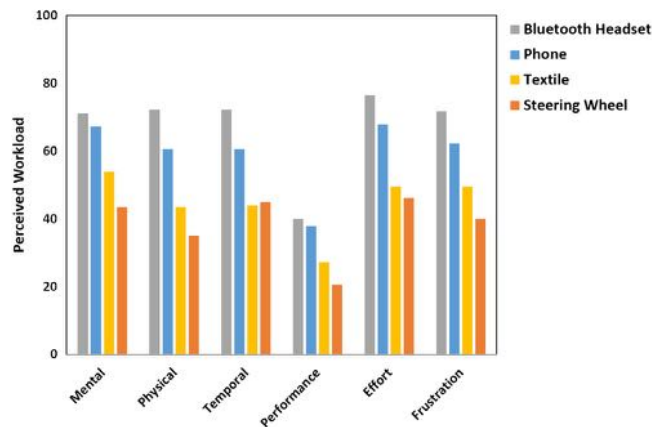**Fig. 14.** Secondary task results: Accuracy (left) and Reaction Time (right).

Fig. 15. Overall perceived workload for different input devices: Phone, Bluetooth headset, Steering wheel, and Textile.

In Fig. 15, the perceived workload difference for each input device is shown. Although participants show good task performances with Bluetooth headset, the perceived workload is the highest. This aligns with the user comments that they were uncomfortable with controlling the headset which were worn around the neck. Participants report that they have to check every button to trigger the proper one. This was also observed during the user study where most users exhibited rubbing motion on the Bluetooth headset before pushing the button. Phone shows high workload rating next to Bluetooth headset. This is due to the fact that phone requires eyes-on interaction unlike other devices. All participants report that they have to concentrate very hard onto the display in order to keep track of the primary task while completing the secondary task. Steering wheel exhibits the lowest workload among all devices. Easily approachable button location appeals to most participants. However, some participants comment that the steering wheel cannot be a universal input device since it only works within the car.

Our prototype shows lower workload than Bluetooth headset and phone, but slightly higher workload than the steering wheel. Most participants like that they could easily locate where to press based on their own proprioception. This leads to the lowest workload regarding 'Temporal' for our prototype comparing to other devices. However, participants still comment that it causes some level of workload due to following reasons. First, few users state that the fitting of the prototype is not optimized for each individual. They report that uncomfortable wearability increases the workload regarding to 'Physical' and 'Performance'. Furthermore, one user mention that the fabric knots from the sensing area causes a minor pain over the time and his long thumb prevents him from triggering the inner pressure sensing. We assume this affects 'Frustration', 'Effort', and 'Mental' workload components.

The positive comments about the proposed input device include:

"I like that I can control the mobile application right away without wearing a huge device"
"It is convenient to control music without looking at anything"
"Since I was pressing on my own finger, I had an idea where I was supposed to press without looking after a time"
"I moved my fingers less than smartphone and Bluetooth devices"

Users favor on the eyes-free feature and simple working principles of the proposed prototype with less required motion. Users also like the form factor which encourages the use of proprioception and natural haptic feedback at the finger. The need-to-improve feedback include:

"The Finger glove seems to be slippery. When I tried to perform swipe gesture, the glove got wear off few times".
"I do not have to look at the finger while controlling, but I need to look at the phone for information from time to time"
"It starts to hurt as I select some buttons due to fabric knots"

From user feedback, we find out that all users favor in the eyes-free feature in mobile interaction. Comparatively low perceived workload show that the prototype has a potential to reduce physical/cognitive costs as a new input device. User's comments also imply that the prototype still has a room to further bringing down the cognitive load with hardware and software improvements.

5. Future work and conclusion

We use conductive threads to provide a soft conductive path in our current design. In our next step, we plan to explore the ink-jet printing technology with textiles to further improve the fabrication process. For better accuracy, we consider using supervised learning method like Support Vector Machine (SVM). The signal from the finger bending shows a potential to be used as a unique feature for different input controls. For example, the natural finger bending angle is different when activating inner and outer pressure sensing spots. In order to understand the habitual motion better and increase the robustness, we plan to collect and analyze larger number of samples. It is also in our interest to mitigate the ambient activity by fusing additional sensors like accelerometer and gyroscope. Future designs embedding higher sensitivity for bending with deeper ergonomic considerations will bring out additional user experiences based on our initial work. Lastly, it will be interesting to apply our proposed work in other application area such as input device for blind people.

We demonstrate a finger-worn textile input device with multimodal sensing capabilities for eyes-free mobile interaction during daily activities. We implemented pressure and strain sensor on a single layer of fabric by painting carbon elastomer and stitching conductive threads. We conducted both quantitative and qualitative user studies to evaluate the prototype's system performance as well as comparative workload. The performance evaluations verify that the prototype is robust against physical interferences and motion artifacts while causing only a few accidental triggers during various activities. The eyes-free interaction with 3-button UI shows an acceptable performance of the proposed work (88%). The multitasking study verifies that our prototype is less susceptible to the visual distraction comparing with other conventional input devices. The implemented application and user feedback conclusively show that participants favor the eyes-free mobile interaction with the wearable input device. We expect that our work will benefit in exploiting smart textiles as a multimodal input device which supports an eyes-free mobile interaction during daily activities.

Acknowledgments

References

[1] J. Han, L. Shao, D. Xu, J. Shotton, Enhanced computer vision with microsoft kinect sensor: A review.
[2] D. Tong, K. Bartels, K. Honeyager, Adaptive reduction of motion artifact in the electrocardiogram, in: Engineering in Medicine and Biology, 2002. 24th Annual Conference and the Annual Fall Meeting of the Biomedical Engineering Society EMBS/BMES Conference, 2002. Proceedings of the Second Joint, Vol. 2, IEEE, 2002, pp. 1403–1404.
[3] B. Yi, X. Cao, M. Fjeld, S. Zhao, Exploring user motivations for eyes-free interaction on mobile devices, in: Proceedings of the SIGCHI Conference on Human Factors in Computing Systems, ACM, 2012, pp. 2789–2792.

[4] S. Brewster, J. Lumsden, M. Bell, M. Hall, S. Tasker, Multimodal'eyes-free'interaction techniques for wearable devices, in: Proceedings of the SIGCHI conference on Human Factors in Computing Systems, ACM, 2003, pp. 473–480.

[5] D.L. Ashbrook, J.R. Clawson, K. Lyons, T.E. Starner, N. Patel, Quickdraw: the impact of mobility and on-body placement on device access time, in: Proceedings of the SIGCHI Conference on Human Factors in Computing Systems, ACM, 2008, pp. 219–222.

[6] K. Hinckley, J. Pierce, M. Sinclair, E. Horvitz, Sensing techniques for mobile interaction, in: Proceedings of the 13th Annual ACM Symposium on User Interface Software and Technology, ACM, 2000, pp. 91–100.

[7] G. Cho, Smart Clothing: Technology and Applications, CRC Press, 2010 (chapter 9).

[8] J. Meyer, B. Arnrich, J. Schumm, G. Troster, Design and modeling of a textile pressure sensor for sitting posture classification, Sensors J. 10 (8) (2010) 1391–1398.

[9] L.M. Castano, A.B. Flatau, Smart fabric sensors and e-textile technologies: a review, Smart Mater. Struct. 23 (5) (2014) 053001.

[10] F. Gonzalez, F. Gosselin, W. Bachta, A framework for the classification of dexterous haptic interfaces based on the identification of the most frequently used hand contact areas, in: World Haptics Conference (WHC), IEEE, 2013, pp. 461–466.

[11] L. Chan, R.-H. Liang, M.-C. Tsai, K.-Y. Cheng, C.-H. Su, M.Y. Chen, W.-H. Cheng, B.-Y. Chen, Fingerpad: private and subtle interaction using fingertips, in: Proceedings of the 26th Annual ACM Symposium on User Interface Software and Technology, ACM, 2013, pp. 255–260.

[12] M. Ogata, Y. Sugiura, H. Osawa, M. Imai, iring: intelligent ring using infrared reflection, in: Proceedings of the 25th Annual ACM Symposium on User Interface Software and Technology, ACM, 2012, pp. 131–136.

[13] K. Tsukada, M. Yasumura, Ubi-finger: gesture input device for mobile use, in: Proceedings of APCHI, Vol. 1, 2002. pp. 388-400.

[14] X.-D. Yang, T. Grossman, D. Wigdor, G. Fitzmaurice, Magic finger: always-available input through finger instrumentation, in: Proceedings of the 25th Annual ACM Symposium on User Interface Software and Technology, ACM, 2012, pp. 147–156.

[15] S.H. Yoon, K. Huo, K. Ramani, Plex: finger-worn textile sensor for mobile interaction during activities, in: Proceedings of the 2014 ACM International Joint Conference on Pervasive and Ubiquitous Computing: Adjunct Publication, ACM, 2014, pp. 191–194.

[16] S.H. Yoon, K. Huo, V.P. Nguyen, K. Ramani, Timmi: finger-worn textile input device with multimodal sensing in mobile interaction, in: Proceedings of the Ninth International Conference on Tangible, Embedded, and Embodied Interaction, ACM, 2015, pp. 269–272.

[17] D.L. Ashbrook, J.R. Clawson, K. Lyons, T.E. Starner, N. Patel, Quickdraw: the impact of mobility and on-body placement on device access time, in: Proceedings of the SIGCHI Conference on Human Factors in Computing Systems, ACM, 2008, pp. 219–222.

[18] T. Karrer, M. Wittenhagen, L. Lichtschlag, F. Heller, J. Borchers, Pinstripe: eyes-free continuous input on interactive clothing, in: Proceedings of the SIGCHI Conference on Human Factors in Computing Systems, ACM, 2011, pp. 1313–1322.

[19] D. Ashbrook, P. Baudisch, S. White, Nenya: subtle and eyes-free mobile input with a magnetically-tracked finger ring, in: Proceedings of the SIGCHI Conference on Human Factors in Computing Systems, ACM, 2011, pp. 2043–2046.

[20] P. Mistry, P. Maes, Sixthsense: a wearable gestural interface, in: ACM SIGGRAPH ASIA 2009 Sketches, ACM, 2009, p. 11.

[21] J. Rekimoto, Gesturewrist and gesturepad: unobtrusive wearable interaction devices, in: Wearable Computers, 2001. Proceedings. Fifth International Symposium on, IEEE, 2001, pp. 21–27.

[22] C. Harrison, D. Tan, D. Morris, Skinput: appropriating the body as an input surface, in: Proceedings of the SIGCHI Conference on Human Factors in Computing Systems, ACM, 2010, pp. 453–462.

[23] D. Morris, T.S. Saponas, D. Tan, Emerging input technologies for always-available mobile interaction, Found. Trends Human Comput. Interact. 4 (4) (2011) 245–316.

[24] C. Cochrane, V. Koncar, M. Lewandowski, C. Dufour, Design and development of a flexible strain sensor for textile structures based on a conductive polymer composite, Sensors 7 (4) (2007) 473–492.

[25] F. Lorussi, W. Rocchia, E.P. Scilingo, A. Tognetti, D. De Rossi, Wearable, redundant fabric-based sensor arrays for reconstruction of body segment posture, Sensors J. 4 (6) (2004) 807–818.

[26] M. Shimojo, A. Namiki, M. Ishikawa, R. Makino, K. Mabuchi, A tactile sensor sheet using pressure conductive rubber with electrical-wires stitched method, Sensors J. 4 (5) (2004) 589–596.

[27] K. Huber, M. Salmani, Y. Fernaeus, The making of the teleglove: crafting interactions for basic phone use in the cold, in: Proceedings of the 8th International Conference on Tangible, Embedded and Embodied Interaction, ACM, 2014, pp. 241–244.

[28] Blue infusion Technologies, Beartek glove, retrieved January 10, 2016 from http://www.beartekgloves.com, 2013.

[29] K. Willms, R. Wells, H. Carnahan, Glove attributes and their contribution to force decrement and increased effort in power grip at maximal and submaximal levels, Human Fact. J. Human Factors Ergon. Soc.

[30] P. Haggard, J.R. Flanagan, Hand and Brain: the Neurophysiology and Psychology of Hand Movements, Academic Press, 1996.

[31] T.S. Saponas, C. Harrison, H. Benko, Pockettouch: through-fabric capacitive touch input, in: Proceedings of the 24th Annual ACM Symposium on User Interface Software and Technology, ACM, 2011, pp. 303–308.

[32] S. Zhao, P. Dragicevic, M. Chignell, R. Balakrishnan, P. Baudisch, Earpod: eyes-free menu selection using touch input and reactive audio feedback, in: Proceedings of the SIGCHI Conference on Human Factors in Computing Systems, ACM, 2007, pp. 1395–1404.

[33] C. Harrison, B.Y. Lim, A. Shick, S.E. Hudson, Where to locate wearable displays?: reaction time performance of visual alerts from tip to toe, in: Proceedings of the SIGCHI Conference on Human Factors in Computing Systems, ACM, 2009, pp. 941–944.

[34] H.P. Profita, J. Clawson, S. Gilliland, C. Zeagler, T. Starner, J. Budd, E. Y.-L. Do, Don't mind me touching my wrist: a case study of interacting with on-body technology in public, in: Proceedings of the 17th Annual International Symposium on International Symposium on Wearable Computers, ACM, 2013, pp. 89–96.

[35] J.N. Ingram, K.P. Körding, I.S. Howard, D.M. Wolpert, The statistics of natural hand movements, Exp. Brain Res. 188 (2) (2008) 223–236.

[36] S.N. Imrhan, Trends in finger pinch strength in children, adults, and the elderly, Human Fact. J. Human Factors Ergon. Soc. 31 (6) (1989) 689–701.

[37] Wacker, LR3162, retrieved January 10, 2016 from http://www.wacker.com, 2012.

[38] Sparkfun, Microview, retrieved January 10, 2016 from http://www.sparkfun.com/products/12923, 2013.

[39] Z. Del Prete, L. Monteleone, R. Steindler, A novel pressure array sensor based on contact resistance variation: metrological properties, Rev. Sci. Instrum. 72 (2) (2001) 1548–1553.

[40] D.L. Lee, H. McLoone, J.T. Dennerlein, Observed finger behaviour during computer mouse use, Appl. Ergon. 39 (1) (2008) 107–113.

[41] D. Kim, O. Hilliges, S. Izadi, A.D. Butler, J. Chen, I. Oikonomidis, P. Olivier, Digits: freehand 3d interactions anywhere using a wrist-worn gloveless sensor, in: Proceedings of the 25th Annual ACM Symposium on User Interface Software and Technology, ACM, 2012, pp. 167–176.

[42] K. Lyngsie, M.S. Pedersen, J. Stage, K.F. Vestergaard, Don't text while driving: the effect of smartphone text messaging on road safety during simulated driving, in: Human-Computer Interaction–INTERACT 2013, Springer, 2013, pp. 546–563.

[43] Thalmic Lab, Myo armband, retrieved January 10, 2016 from https://www.myo.com, 2014.

[44] E.H. Schumacher, T.L. Seymour, J.M. Glass, D.E. Fencsik, E.J. Lauber, D.E. Kieras, D.E. Meyer, Virtually perfect time sharing in dual-task performance: uncorking the central cognitive bottleneck, Psychol. Sci. 12 (2) (2001) 101–108.

[45] S.C. Lee, T. Starner, Buzzwear: alert perception in wearable tactile displays on the wrist, in: Proceedings of the SIGCHI Conference on Human Factors in Computing Systems, ACM, 2010, pp. 433–442.

[46] S.G. Hart, L.E. Staveland, Development of nasa-tlx (task load index): results of empirical and theoretical research, Adv. Psychol. 52 (1988) 139–183.